Acta Cryst. (1989). B45, 423–431

The Location of *p*-Xylene in a Single Crystal of Zeolite H-ZSM-5 with a New, Sorbate-Induced, Orthorhombic Framework Symmetry

BY H. VAN KONINGSVELD AND F. TUINSTRA

Laboratory of Applied Physics, Delft University of Technology, Lorentzweg 1, 2628 *CJ Delft, The Netherlands*

AND H. VAN BEKKUM AND J. C. JANSEN

Laboratory of Organic Chemistry, Delft University of Technology, Julianalaan 136, 2628 *BL Delft, The Netherlands*

(*Received* 27 *January* 1989; *accepted* 4 *April* 1989)

Abstract

$Si_{23.92}Al_{0.08}O_{48}.2C_8H_{10}$ $(+0.08H^+)$, $M_r = 1654.26$, orthorhombic, $P2_12_12_1$, $a = 20.121$ (1), $b = 19.820$ (1), $c = 13.438$ (1) Å, $V = 5359$ (3) Å^3, $Z = 4$, $D_x^* = 2.06$ (including *p*-xylene), $D_x = 1.80$ g cm^{-3} (for the framework), λ(Cu $K\alpha$) = 1.54180 Å, $\mu = 62.7$ cm^{-1}, $F(000) = 3343.7$, $T = 293$ K, $R = 0.039$ for 5796 observed reflections with $I > 1.0\sigma(I)$. The adsorption of *p*-xylene in the sinusoidal channels is accompanied by a cooperative deformation of the (100) pentasil layers. The resulting strictly alternating shift of adjacent (010) pentasil layers along **c** changes the monoclinic H-ZSM-5 framework to orthorhombic symmetry with space group $P2_12_12_1$. This space group is different from the orthorhombic space group of as-synthesized ZSM-5 (*Pnma*) and has not been reported before. The straight channel parallel to [010] is slightly corrugated. The elliptical cross section has limiting ports of about 6.1 × 4.8 Å. The sinusoidal channel, parallel to [100], is elliptical with major and minor axes of about 6.2 and 4.6 Å, respectively. One of the two independent *p*-xylene molecules lies at the intersection of the straight and the sinusoidal channels with its long molecular axis nearly parallel to the straight channel axis. The second *p*-xylene molecule is in the sinusoidal channel with its long molecular axis nearly parallel to [100]. The minimal cross section of the *p*-xylene molecules fills the maximal limiting ports in both channels. The molecule in the sinusoidal channel is more tightly constricted by the framework atoms than the molecule in the straight channel. The main interaction forces between the *p*-xylene molecule at the intersection of channels and the one in the sinusoidal channel are almost identical to those in the (001) and ($\bar{1}04$) layers of *p*-xylene and α-toluene single crystals, respectively. A detailed comparison of the pore sizes in the frameworks of as-synthesized ZSM-5 (*Pnma*), H-ZSM-5 ($P2_1/n$) and of the *p*-xylene/H-ZSM-5 complex ($P2_12_12_1$) is made and a sorption mechanism is discussed.

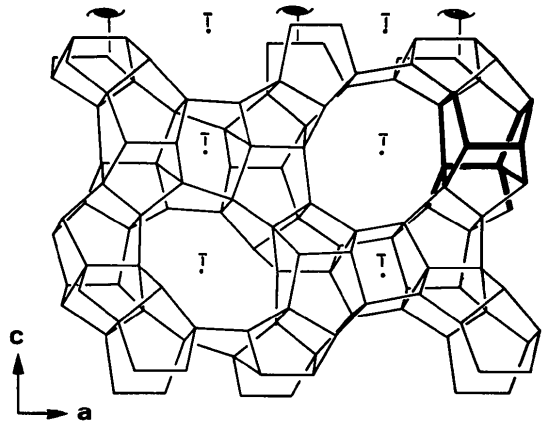

Fig. 1. Characteristic (010) pentasil layer in as-synthesized orthorhombic ZSM-5. *T* atoms are at intersections of lines. O atoms (not drawn) are about midway between *T* atoms. A T_{12} building unit is indicated by bold lines.

Introduction

The catalytic and shape-selective properties of microporous crystalline aluminosilicates are closely related to their framework structure of cages and channels.

The framework of as-synthesized ZSM-5 has orthorhombic *Pnma* symmetry (Wu, Lawton, Olson, Rohrman & Kokotailo, 1979) and can be built up in the following way. A building unit, containing 12 *T* sites (T = Si, Al) is shown in Fig. 1. The (010) pentasil layer with the T_{10} rings of the straight channel (Fig. 1) is generated by applying successively a twofold screw operation and an inversion to the building unit. The three-dimensional framework is completed by linking neighbouring (010) layers by reflection. Thereby, a second type of pentasil layers is generated. One of these (100) pentasil layers, containing the sinusoidal double T_{10}-ring channels, is shown in Fig. 2(*a*). A detailed structure analysis of the occluded template ion, tetrapropylammonium (TPA), in as-synthesized ZSM-5 (van Koningsveld, van Bekkum & Jansen, 1987)

0108-7681/89/040423-09$03.00

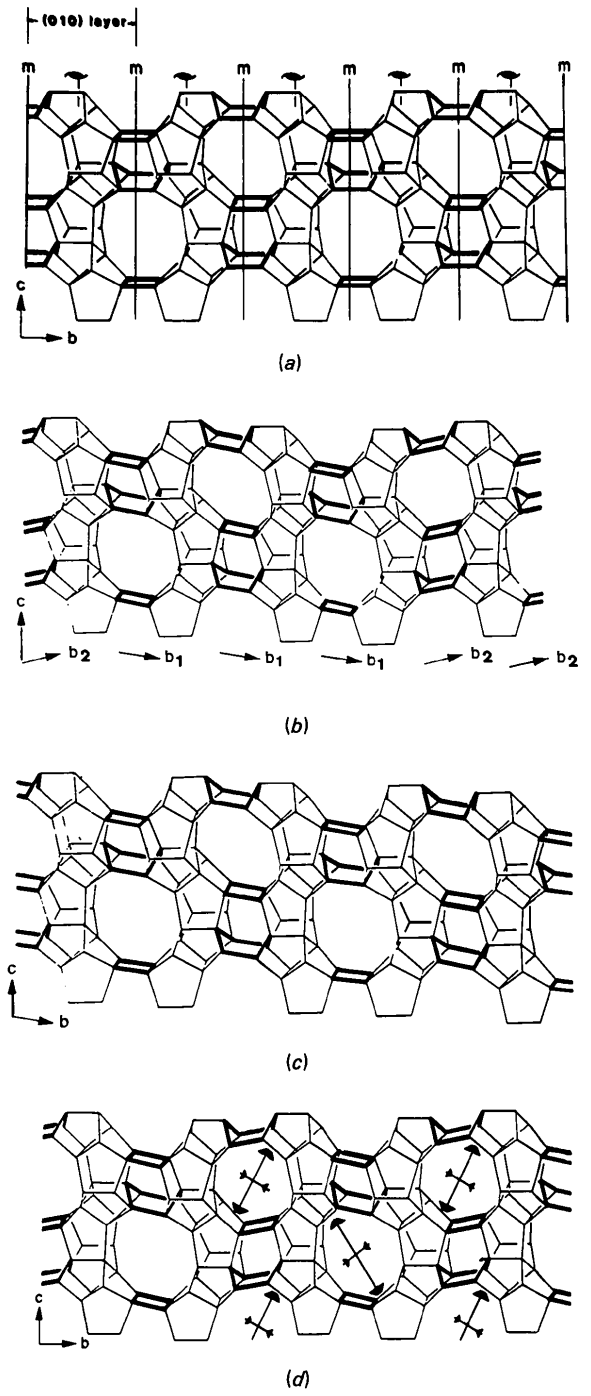

Fig. 2. (*a*) (100) pentasil layer in orthorhombic as-synthesized ZSM-5 as well as in ORTHO (assumed). (*b*) (100) pentasil layer in monoclinic H-ZSM-5 at room temperature. Random (exaggerated) shift of (010) layers along +**c** and −**c**. [Note: in the actual crystal the size of the twin domains is at least 50 unit cells (≃1000 Å)]. (*c*) As (*b*) but *after* application of mechanical stress. A (perfect) monoclinic single crystal (MONO) is shown. (*d*) (100) pentasil layer in PARA, showing the strictly alternating shift of successive (010) layers along **c**. Arrows indicate the direction of the deformation of the framework upon adsorption of *p*-xylene (see last section of *Discussion*).

showed that TPA is located at the intersection of the straight and sinusoidal channels.

H-ZSM-5, obtained by calcination of as-synthesized ZSM-5 followed by NH_4^+ exchange and a second calcination, shows a reversible structural phase transition at about 340 K (the precise temperature being dependent on the Al content) and exhibits monoclinic symmetry below and orthorhombic symmetry above the transition temperature (Hay & Jaeger, 1984; Hay, Jaeger & West, 1985; Klinowski, Carpenter & Gladden, 1987). The high-temperature orthorhombic H-ZSM-5 phase (hereafter called ORTHO) is assumed to have the same space group as the as-synthesized ZSM-5 crystal (*Pnma*; Fig. 2*a*). Upon cooling, ORTHO changes into an aggregate of twin domains with monoclinic $P2_1/n.1.1$ symmetry. The twin formation can be ascribed to a mutual shift of successive (010) layers along +**c** or −**c** as shown in Fig. 2(*b*) (van Koningsveld, Jansen & van Bekkum, 1987). Monoclinic H-ZSM-5 appears to be ferroelastic: application of an appropriate uniaxial mechanical stress changes the population of the twin domains (van Koningsveld, Tuinstra, Jansen & van Bekkum, 1989). An X-ray analysis of a monoclinic (nearly) single crystal of H-ZSM-5 (hereafter called MONO; Fig. 2*c*) revealed that the MONO framework is less strained than the ORTHO framework (van Koningsveld, Jansen & van Bekkum, 1989).

At room temperature, the phase transition can be reversibly induced by loading/unloading H-ZSM-5 powder with NH_3 (Wu *et al.*, 1979) and with various organic molecules (Fyfe, Kennedy, de Schutter & Kokotailo, 1984; Kokotailo, Fyfe, Kennedy, Gobbi, Strobl, Pasztor, Barlow, Bradley, Murphy & Ozubko, 1986; Olson, Kokotailo, Lawton & Meier, 1981). The sorbate-loaded and -unloaded H-ZSM-5 shows orthorhombic and monoclinic symmetry, respectively.

Very recently, adsorption/desorption isotherms of *p*-xylene in H-ZSM-5 (Si/Al = 132) at 313 and 323 K were published (Richards & Rees, 1988). For sorbate loadings greater than 4 molecules per unit cell the sudden increase of the adsorption from 4 to 7·6 molecules per unit cell, at constant P/P_0, as well as the hysteresis loop, earlier described by Olson *et al.* (1981), were observed. A maximum adsorption capacity between 5·8 and 8 molecules of *p*-xylene per unit cell at ~ 300 K was reported for silicalite (Thamm, 1987) and H-ZSM-5 powder samples (Olson *et al.*, 1981; Andersen, Foger, Mole, Rajadhyaksha & Sanders, 1979; Derouane & Gabelica, 1980). In this 'high-coverage' *p*-xylene/H-ZSM-5 complex, the *p*-xylene molecules were localized by X-ray powder diffraction analysis, assuming orthorhombic *Pnma* symmetry (Mentzen, Bosselet & Bouix, 1987). In the straight channel, four *p*-xylene molecules are at the intersection of channels with their long molecular axis perpendicular to the crystallographic mirror plane *m* and with their molec-

ular centre in *m*. In the sinusoidal channel, the other four *p*-xylene molecules have their molecular plane coincident with the crystallographic mirror plane.

Above the transition temperature the maximal adsorption capacity of H-ZSM-5 is near 4 molecules per unit cell (Olson *et al.*, 1981). A 'low-coverage' loading of *p*-xylene is also achieved by adsorption of *p*-xylene vapor at low pressure at room temperature (Mentzen, 1987*a*,*b*). X-ray powder diffraction analysis revealed a disordered *p*-xylene molecule at the intersection of channels with its long molecular axis parallel to the straight channel axis and its centroid in the mirror plane of the space group *Pnma* (Mentzen & Vigné-Maeder, 1987).

Analogous positions of *p*-xylene in the 'high-coverage' and 'low-coverage' complexes were recently predicted by a packing analysis (Reischman, Schmitt & Olson, 1988) using the *PCK*6 program of Williams (1969, 1972). No specific symmetry relations between the adsorbed molecules were presumed. The framework was not allowed to change and had *Pnma* symmetry. Experimentally, by applying ^{13}C MAS NMR, the authors were able to distinguish two types of adsorbed *p*-xylene molecules.

The present paper reports on the structure analysis of single crystals of the high-coverage *p*-xylene/H-ZSM-5 complex (hereafter called PARA) with the orthorhombic space group $P2_12_12_1$. This space group is different from that of ORTHO and has not been reported before. We show that the shift of (010) pentasil layers along $+\mathbf{c}$ and $-\mathbf{c}$, also responsible for the ORTHO–MONO transition, is now strictly alternating (Fig. 2*d*); we analyse the role of *p*-xylene in this process. It is the first detailed structural study of a sorbate in a crystal of H-ZSM-5 using single-crystal X-ray diffraction methods.

Experimental

ZSM-5 crystals were obtained as described recently (Lermer, Draeger, Steffen & Unger, 1985) and subsequently converted into H-ZSM-5 (van Koningsveld, Jansen & van Bekkum, 1987). A freshly prepared H-ZSM-5 crystal (with Si/Al $\simeq$ 300), having approximate dimensions 125 × 100 × 225 μm in **a**, **b** and **c** directions, respectively, was saturated with *p*-xylene vapour while cooling down from about 400 K to room temperature within 10 min. The cell parameters of PARA were obtained by least-squares fitting of four alternative settings of 25 reflections in the range $23 < \theta < 30°$, with the 'set 4' method of de Boer & Duisenberg (1984). The systematic extinctions were consistent with the space group $P2_12_12_1$. The unloaded H-ZSM-5 crystal is a monoclinic microtwinned crystal. Therefore, PARA could be twinned as well. Intensities were measured to $\theta_{max} = 76{\cdot}0°$ with an $\omega/2\theta$ scan, scan width $= (0{\cdot}85 + 0{\cdot}15\tan\theta)°$, on a CAD-4 diffractometer using graphite-monochromated Cu $K\alpha$ radiation ($h_{max} = 25$, $k_{max} = 25$, $l_{max} = 16$). The intensities were measured with 2% accuracy or for a maximum counting time of 120 s. Three reference reflections were measured every 2 h of X-ray measuring time; no systematic change in intensity was observed. Lorentz and polarization corrections were applied but none for extinction or absorption. A unique data set of 6144 reflections, of which 5858 had $I > \sigma(I)$, was obtained. The initial positions of the framework atoms for PARA were taken from MONO (van Koningsveld, Jansen & van Bekkum, 1989). For a direct comparison of the ORTHO, MONO and PARA structures, it is necessary to shift the origin in the standard $P2_12_12_1$ setting to $(0, 0, \frac{1}{4})$.* All *T* atoms (Si, Al) were treated as Si. The framework structure was refined in $P2_12_12_1$ by isotropic refinement on *F* to $R = 0{\cdot}12$. At this stage a difference Fourier map clearly showed two independent *p*-xylene molecules. Isotropic refinement, including *p*-xylene, converged to $R = 0{\cdot}069$ using all 5858 observed reflections. The population parameters, one for each *p*-xylene molecule, were refined to 1·07 (2) and 1·09 (1). These values were reset to 1·00 and kept fixed in the subsequent refinement cycles. Anisotropic refinement of the framework atoms lowered *R* to 0·053; inclusion of anisotropic movement of *p*-xylene gave $R = 0{\cdot}045$. Inspection of the structure-factor table showed poor agreement between F_{obs} and F_{calc} for 62 reflections with *h*, or *k*, or $l \leq 3$. These reflections were suspected of being seriously affected by coherent scattering of the twin domains and/or absorption effects and were left out of the final refinement cycles. The final $R = 0{\cdot}039$, $wR = 0{\cdot}041$ ($w = 1$) and $S = 1{\cdot}04$ for 794 variables and 5998 observations [5796 with $I > \sigma(I)$ plus those for which $F_c > F_o$]. The average and maximum shift/e.s.d. were 0·16 and 1·5 [U_{11} of Si(5)], respectively. The final ΔF synthesis had $\rho < 0{\cdot}51$ e Å^{-3} with peaks in close vicinity of the framework atoms. The synthesis is featureless elsewhere. All calculations were performed on the Delft University Amdahl 470/V7B computer using programs of the *XRAY*72 system (Stewart, Kruger, Ammon, Dickinson & Hall, 1972); atomic scattering factors of zero-valent Si, O and C from Cromer & Mann (1968) were used. Final positional and thermal parameters of the framework and the sorbate molecules are given in Tables 1 and 2, respectively.

After storage for half a year at 295 K and atmospheric pressure, the PARA crystal was remeasured at 295 K using Mo radiation and subsequently refined with the same set of reflections to $R = 0{\cdot}037$.† The PARA geometry does not change

*The symmetry operations in $P2_12_12_1$ become: x, y, z; $x+\frac{1}{2}, \frac{1}{2}-y, \frac{1}{2}-z$; $-x, y+\frac{1}{2}, -z$ and $\frac{1}{2}-x, -y, \frac{1}{2}+z$.

†The agreement between F_{obs} and F_{calc} of 29 of the 62 ignored reflections was significantly improved compared to the Cu refinement.

significantly: corresponding distances and angles from both measurements are equal within 3σ.

Discussion

Geometry of the zeolite framework

Distances and angles are summarized in Table 3,* together with the corresponding values in MONO and ORTHO. The range of OSiO angles is about equal in all three structures. The SiO_4 groups agree well with the ideal tetrahedral environment of Si atoms; the average OSiO angle in each tetrahedron is 109·47°, without any significant scatter. The minimum value of the Si—O distance [d(Si—O)] in PARA lies between the corresponding values in ORTHO and MONO; the maximum value is essentially the same in all three frameworks. The range of the average d(Si—O) in the tetrahedra is equal in PARA and MONO and slightly smaller in ORTHO. Fig. 3 gives the scatter diagram of $\langle d(\text{Si—O})\rangle$, the average d(Si—O) in an Si—O—Si bridge, plotted as a function of the SiOSi angle. Smaller $\langle d(\text{Si—O})\rangle$ involve wider SiOSi angles, in agreement with findings in some silica polymorphs (Hill & Gibbs, 1979) and with semi-empirical molecular-orbital calculations (Tossell & Gibbs, 1978). From the difference in slope of the regression lines in MONO and ORTHO it was concluded (van Koningsveld, Jansen & van Bekkum, 1989) that the MONO framework is the less-strained one. (The ORTHO framework is assumed to have the same geometry as the as-synthesized TPA-ZSM-5 framework.) The difference between the dependence of $\langle d(\text{Si—O})\rangle$ on SiOSi in PARA and MONO is much less pronounced and the orthorhombic PARA framework seems hardly more strained than the monoclinic MONO framework.

A comparison between the pore openings in the T_{10} rings in the channels down [010] and [100], described by their 'diagonal' O···O distances, is given in Table 7. The symmetry change between ORTHO and MONO hardly affects the pore size in the straight channel. The free area in each 10-ring in the sinusoidal double 10-ring, however, changes from nearly circular to a more elliptical form. The sinusoidal channel in MONO therefore becomes more accessible to *p*-xylene than the sinusoidal channel in ORTHO. The pore sizes in PARA again have changed drastically and are about equal in both channel systems. The change in pore dimensions upon adsorption of *p*-xylene explains why the effective cross sections seem to be larger than those calculated from a rigid framework (Wu, Landolt & Chester, 1986). A detailed discussion on the pore sizes in connection with a possible sorption mechanism is given in the last section.

Table 1. *Fractional coordinates* ($\times 10^4$) *and* U_{eq} *values* ($Å^2 \times 10^3$) *for the framework atoms in PARA*

$U_{eq} = \frac{1}{3}(U_{11} + U_{22} + U_{33})$.

	x	y	z	U_{eq}
Si(1)	4251·2 (7)	661·4 (7)	−2965·9 (10)	9·6 (4)
Si(2)	3176·5 (7)	317·1 (7)	−1471·7 (10)	10·3 (4)
Si(3)	2798·3 (7)	529·0 (7)	741·6 (10)	10·8 (4)
Si(4)	1232·2 (7)	546·8 (7)	660·5 (10)	10·4 (4)
Si(5)	758·6 (7)	295·7 (7)	−1527·8 (11)	10·7 (4)
Si(6)	1962·7 (7)	705·2 (6)	−2806·2 (10)	9·3 (4)
Si(7)	4277·5 (7)	−1690·8 (7)	−2922·7 (11)	10·6 (4)
Si(8)	3176·1 (7)	−1278·1 (7)	−1495·0 (11)	11·2 (4)
Si(9)	2732·2 (7)	−1737·8 (7)	604·3 (11)	9·5 (4)
Si(10)	1185·2 (7)	−1747·9 (7)	588·3 (11)	10·7 (4)
Si(11)	743·8 (7)	−1288·3 (7)	−1520·2 (11)	10·7 (4)
Si(12)	1956·7 (7)	−1728·8 (7)	−2799·6 (10)	10·2 (4)
Si(13)	4253·1 (7)	4495·2 (8)	−3429·7 (10)	10·1 (4)
Si(14)	3144·5 (7)	4710·4 (7)	−1901·7 (11)	11·2 (4)
Si(15)	2790·4 (7)	4274·1 (7)	216·2 (11)	10·4 (4)
Si(16)	1214·9 (7)	4268·3 (7)	228·5 (11)	9·7 (4)
Si(17)	743·1 (7)	4689·2 (7)	−1877·1 (11)	9·7 (4)
Si(18)	1924·8 (7)	4498·7 (7)	−3379·6 (10)	10·2 (4)
Si(19)	4280·1 (7)	6740·7 (7)	−3241·0 (11)	10·3 (4)
Si(20)	3171·2 (7)	6277·3 (7)	−1823·6 (11)	10·4 (4)
Si(21)	2747·4 (7)	6719·7 (7)	248·4 (11)	10·6 (4)
Si(22)	1203·5 (7)	6715·0 (7)	246·0 (12)	11·1 (4)
Si(23)	738·4 (7)	6279·3 (7)	−1844·3 (12)	11·1 (4)
Si(24)	1957·8 (7)	6731·9 (7)	−3165·9 (10)	10·5 (4)
O(1)	3855 (2)	610 (2)	−1929 (3)	19 (1)
O(2)	3174 (2)	483 (2)	−305 (3)	20 (1)
O(3)	2019 (2)	543 (3)	539 (3)	31 (1)
O(4)	877 (2)	529 (3)	−402 (3)	29 (2)
O(5)	1263 (2)	676 (2)	−2246 (3)	23 (2)
O(6)	2555 (2)	654 (2)	−2015 (3)	21 (2)
O(7)	3860 (2)	−1576 (2)	−1924 (3)	24 (2)
O(8)	3127 (2)	−1442 (2)	−334 (3)	20 (2)
O(9)	1956 (2)	−1559 (2)	475 (3)	22 (2)
O(10)	792 (2)	−1485 (2)	−373 (3)	28 (2)
O(11)	1290 (2)	−1667 (2)	−2159 (4)	27 (2)
O(12)	2568 (2)	−1626 (3)	−2075 (4)	31 (2)
O(13)	3155 (2)	−481 (2)	−1669 (3)	29 (2)
O(14)	864 (2)	−498 (3)	−1628 (4)	32 (2)
O(15)	4131 (2)	1390 (2)	−3446 (3)	19 (2)
O(16)	3984 (3)	98 (2)	−3718 (4)	29 (2)
O(17)	3985 (2)	−1224 (2)	−3792 (4)	26 (2)
O(18)	2000 (2)	1404 (2)	−3388 (3)	16 (2)
O(19)	2020 (3)	107 (2)	−3593 (3)	28 (2)
O(20)	1969 (3)	−1198 (2)	−3686 (3)	26 (2)
O(21)	22 (2)	491 (3)	−1863 (3)	24 (2)
O(22)	34 (2)	−1507 (2)	−1916 (3)	25 (2)
O(23)	4223 (2)	−2456 (2)	−3284 (4)	26 (2)
O(24)	1975 (2)	−2471 (2)	−3262 (3)	22 (2)
O(25)	2831 (2)	−2531 (2)	673 (3)	19 (2)
O(26)	1099 (2)	−2548 (2)	702 (3)	20 (2)
O(27)	3831 (2)	4527 (3)	−2419 (3)	27 (2)
O(28)	3076 (2)	4285 (2)	−898 (3)	18 (2)
O(29)	1999 (2)	4339 (2)	195 (4)	31 (2)
O(30)	919 (2)	4299 (2)	−867 (3)	23 (2)
O(31)	1259 (2)	4515 (3)	−2733 (3)	24 (2)
O(32)	2550 (2)	4554 (3)	−2660 (3)	29 (2)
O(33)	3871 (2)	6458 (2)	−2315 (3)	25 (2)
O(34)	3116 (2)	6675 (2)	−798 (3)	25 (2)
O(35)	1972 (2)	6552 (2)	89 (4)	32 (2)
O(36)	839 (2)	6663 (2)	−805 (3)	28 (2)
O(37)	1296 (2)	6486 (3)	−2622 (4)	30 (2)
O(38)	2585 (2)	6482 (3)	−2555 (4)	34 (2)
O(39)	3129 (3)	5489 (2)	−1601 (3)	34 (2)
O(40)	754 (2)	5486 (2)	−1654 (3)	27 (2)
O(41)	4097 (3)	3815 (2)	−3988 (4)	37 (2)
O(42)	4078 (3)	5128 (2)	−4122 (4)	29 (2)
O(43)	3999 (2)	6435 (2)	−4268 (3)	19 (2)
O(44)	1951 (2)	3803 (2)	−3979 (3)	21 (2)
O(45)	1912 (2)	5113 (2)	−4155 (3)	22 (2)
O(46)	1984 (2)	6414 (2)	−4262 (3)	20 (2)
O(47)	21 (2)	4452 (2)	−2247 (3)	21 (2)
O(48)	36 (2)	6490 (2)	−2294 (3)	23 (2)

* Lists of structure factors, anisotropic thermal parameters, and bond lengths and bond angles involving framework atoms have been deposited with the British Library Document Supply Centre as Supplementary Publication No. SUP 51773 (37 pp.). Copies may be obtained through The Executive Secretary, International Union of Crystallography, 5 Abbey Square, Chester CH1 2HU, England.

Table 2. *Fractional coordinates* ($\times 10^4$) *and* U_{eq} *values* ($Å^2 \times 10^3$) *of p-xylene molecules at the intersection of channels (XYL1) and in the sinusoidal channel (XYL2)*

$U_{eq} = \frac{1}{3}(U_{11} + U_{22} + U_{33})$.

	x	y	z	U_{eq}
XYL1				
C(10)	5123 (5)	3103 (8)	−333 (9)	80 (6)
C(20)	4817 (6)	2827 (9)	482 (8)	85 (6)
C(30)	4797 (6)	2137 (9)	631 (9)	86 (6)
C(40)	5076 (6)	1657 (9)	−45 (9)	93 (6)
C(50)	5389 (6)	1957 (8)	−877 (9)	83 (6)
C(60)	5424 (5)	2678 (8)	−1000 (8)	79 (6)
C(70)	5152 (9)	3863 (9)	−465 (14)	123 (9)
C(80)	5059 (9)	895 (9)	105 (13)	123 (9)
XYL2				
C(1)	1460 (6)	2481 (4)	−1199 (7)	57 (4)
C(2)	1761 (5)	2842 (4)	−1972 (6)	47 (4)
C(3)	2466 (5)	2876 (4)	−2074 (6)	47 (4)
C(4)	2877 (5)	2557 (4)	−1405 (6)	48 (4)
C(5)	2609 (6)	2211 (5)	−626 (7)	63 (4)
C(6)	1918 (8)	2175 (4)	−513 (7)	76 (5)
C(7)	729 (6)	2429 (6)	−1107 (9)	76 (5)
C(8)	3620 (6)	2604 (6)	−1528 (9)	73 (5)

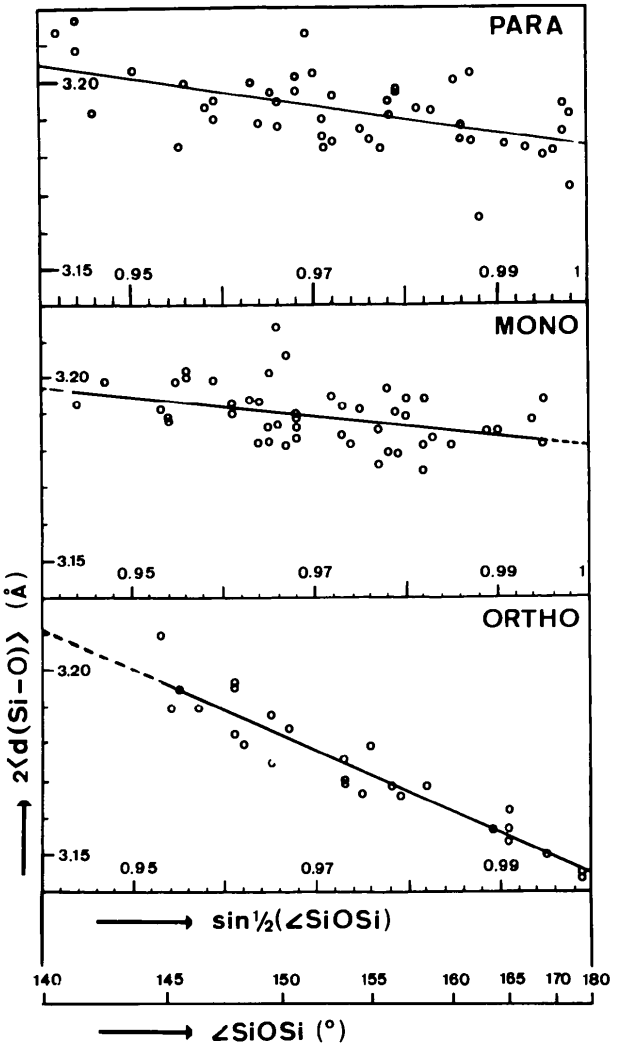

Fig. 3. Scatter diagram of $\langle d(\text{Si–O})\rangle$, plotted as a function of $\sin\frac{1}{2}(\angle\text{SiOSi})$ in ORTHO, MONO and PARA.

Table 3. *Comparison of the framework geometry in PARA, MONO and ORTHO*

	PARA	MONO	ORTHO
O–Si–O range (°)	107·5–112·0 (2)	107·1–111·5 (2)	106·0–112·0 (2)
Av. O–Si–O/SiO_4	109·5	109·5	109·5
Si–O range (Å)	1·574–1·611 (4)	1·582–1·607 (3)	1·567–1·605 (4)
Range of av. Si–O/SiO_4	1·588–1·604	1·588–1·601	1·584–1·591
Si–O–Si range (°)	138·3–172·3 (3)	141·3–169·0 (3)	144·9–175·9 (4)
Range of av. $Si(OSi)_4$	148·5–162·3	147·1–158·8	150·5–162·8

Table 4. *Comparison of bond lengths* (Å) *and bond angles* (°) *in the two p-xylene molecules (XYL1 and XYL2) in H-ZSM-5 with the corresponding values in p-xylene single crystals at* 180 *K (van Koningsveld et al.*, 1986)

	XYL1	XYL2	*p*-Xylene*
Bond lengths			
C(1)–C(2)	1·37 (2)	1·40 (1)	1·394 (2)
C(2)–C(3)	1·38 (3)	1·43 (1)	1·389 (2)
C(3)–C(4)	1·43 (2)	1·38 (1)	1·393 (2)
C(4)–C(5)	1·41 (2)	1·36 (1)	1·394 (2)
C(5)–C(6)	1·44 (2)	1·40 (2)	1·389 (2)
C(6)–C(1)	1·37 (2)	1·44 (2)	1·393 (2)
Mean	1·40	1·40	1·392
C(1)–C(7)	1·52 (3)	1·48 (2)	1·503 (2)
C(4)–C(8)	1·52 (3)	1·51 (2)	1·503 (2)
Mean	1·52	1·50	1·503
Endocyclic angles			
C(1)C(2)C(3)	122 (1)	121·7 (9)	121·0 (1)
C(2)C(3)C(4)	124 (1)	120·8 (8)	121·3 (1)
C(4)C(5)C(6)	122 (1)	120·2 (9)	121·0 (1)
C(5)C(6)C(1)	121 (1)	123·0 (9)	121·3 (1)
Mean	122	121·4	121·2
C(2)C(1)C(6)	118 (2)	114 (1)	117·7 (1)
C(3)C(4)C(5)	113 (2)	120 (1)	117·7 (1)
Mean	116	117	117·7
Exocyclic angles			
C(2)C(1)C(7)	120 (1)	121·8 (10)	121·2 (1)
C(6)C(1)C(7)	121 (1)	123·7 (10)	121·0 (1)
C(3)C(4)C(8)	125 (1)	119·7 (8)	121·2 (1)
C(5)C(4)C(8)	122 (1)	120·6 (9)	121·0 (1)
Mean	122	121·5	121·1

**p*-Xylene has a centre of symmetry.

Geometry and packing of p-xylene

Distances and angles in *p*-xylene, after anisotropic refinement without any constraints on the atoms, are given in Table 4. There are two independent *p*-xylene molecules: XYL1 is located at the intersection of the straight and the sinusoidal channel, XYL2 lies in the sinusoidal channel (Fig. 4). The Me–Me axis (the long axis) in XYL1 deviates about 7·5° from [010] and is nearly parallel to (100). The long axis in XYL2 deviates almost 5·5° from [100] and is practically parallel to (010). The minimal cross section of the *p*-xylene molecules fills the maximal limiting ports in both channels. The mean bond distances and bond angles (Table 4) in both *p*-xylene molecules are in excellent agreement with the corresponding values determined by X-ray analysis of *p*-xylene single crystals (van Koningsveld, van den Berg, Jansen & de Goede, 1986). The

C—C contact between terminal C atoms in neighbouring XYL1 molecules in the straight channel is 4·08 (3) Å. In the sinusoidal channel, the smallest C—C distance between terminal C atoms in adjacent XYL2 molecules is 5·30 (2) Å. The interaction forces between XYL2 molecules are therefore negligible. The packing arrangement of XYL1 and XYL2 molecules is analogous to that observed in layers parallel to (001) and ($\bar{1}$04) in single crystals of *p*-xylene (van Koningsveld *et al.*, 1986) and α-toluene, respectively (Anderson, Bosio, Bruneaux-Poulle & Fourme, 1977).

Table 5. C···H *contacts* (Å) *from* H(*calc.*) *in XYL2 to ring*-C *atoms in XYL1 at room temperature together with the same interactions in single crystals of p-xylene and* α*-toluene at* 180 K

The (methyl) H atom in XYL2 is in a calculated position using values obtained from the (methyl) H atom in the *p*-xylene and α-toluene structures: C—H = 0·98 Å, C—C—H = 114° and CCCH = 24°. E.s.d.'s for C···H ≃ 0·02 Å.

(Me) H in	C(10)	C(20)	C(30)	C(40)	C(50)	C(60)
PARA	3·27	3·19	3·11	3·11	3·15	3·27
p-Xylene	3·18	3·16	3·11	3·07	3·06	3·12
α-Toluene	3·18	3·19	3·13	3·06	3·02	3·09

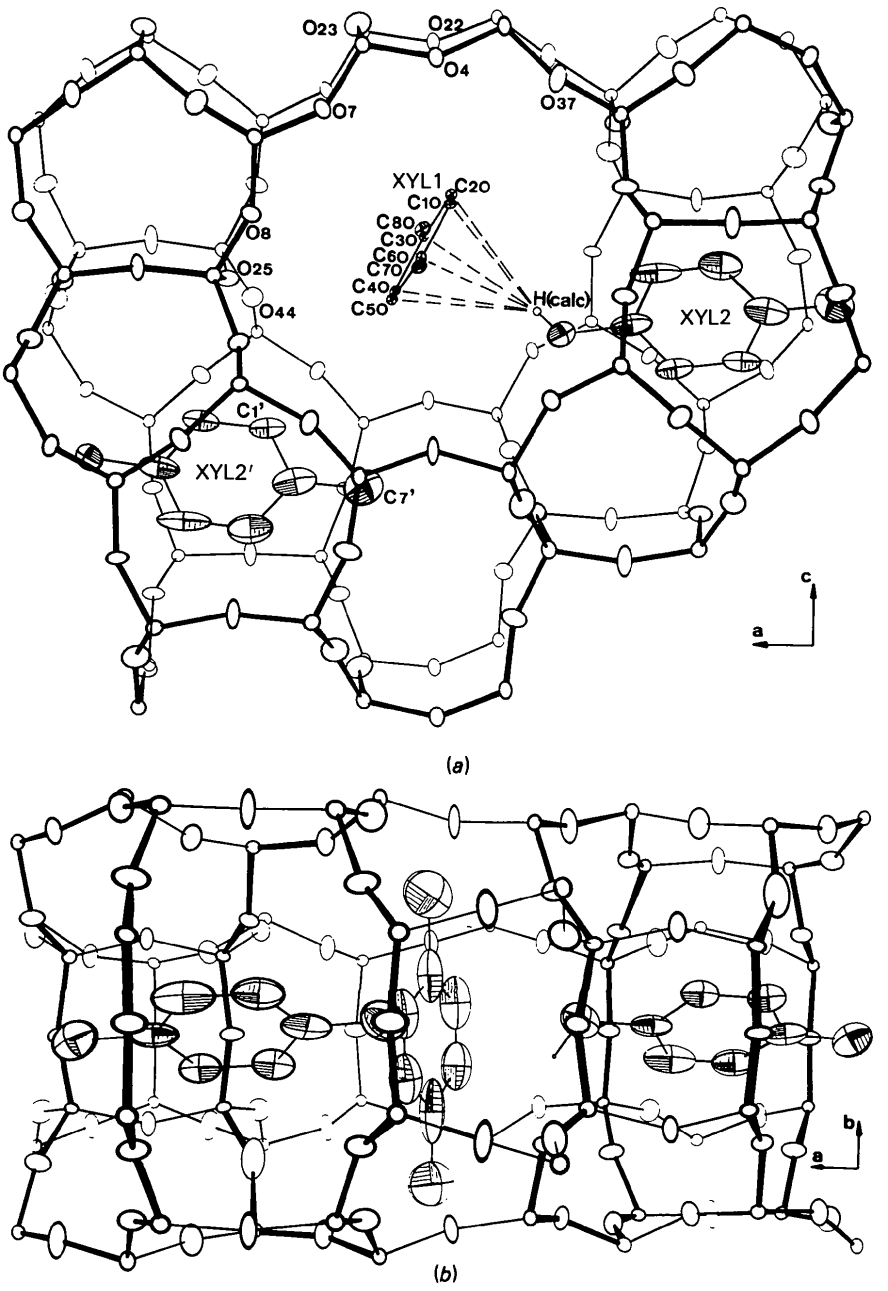

Fig. 4. *ORTEP* drawings (Johnson, 1965) of PARA. (*a*) View down the straight channel axis. XYL1 at intersection of channels; XYL2 and XYL2′ in the sinusoidal channel. H···C interactions shown by dashed lines. (Thermal ellipsoids of XYL1 are scaled down with an arbitrarily chosen factor.) (*b*) View approximately along [001]. Thermal ellipsoids are drawn to enclose 50% probability. The sinusoidal double 10-rings on both sides of the channel intersection are shown as bold lines.

The packing arrangement is described by the H···C contact distances summarized in Table 5 and illustrated for PARA in Fig. 4. The position of the (methyl) H atom in XYL2 is calculated from the *p*-xylene and α-toluene structures (see legend of Table 5). Apparently, the H···aromatic ring contacts represent rather firm interactions. Four short C—C contacts between XYL1 and XYL2′ (symmetry related to XYL2 by a 2_1 axis parallel to **a**), less than 4·3 Å, are given in Table 6 (and Fig. 4) together with short *p*-xylene-to-framework distances less than 3·70 Å. From Table 6 (and Fig. 5) it is seen that the *p*-xylene molecule in the sinusoidal channel (XYL2) is more tightly packed. The closer packing of XYL2 is also apparent from the smaller e.s.d.'s in the observed bond distances and bond angles and from the lower temperature factors [especially the average value of U_{11} of the atoms in XYL2 (~0·10 Å^2) compared with the average value of U_{22} in XYL1 (~0·15 Å^2)].

Table 6. *p-Xylene-to-framework distances* (Å) *less than* 3·70 Å

Some short C—C contacts (<4·3 Å) are added (see text).

XYL1—framework		C(3)—O(32)	3·42 (1)
		—O(44)	3·32 (1)
C(20)—O(7)	3·50 (1)	C(4)—O(28)	3·52 (1)
—O(37)	3·66 (1)	—O(46)	3·54 (1)
—O(48)	3·29 (1)	C(5)—O(2)	3·64 (1)
C(30)—O(22)	3·54 (1)	—O(6)	3·61 (1)
C(50)—O(44)	3·49 (1)	—O(20)	3·40 (1)
C(60)—O(25)	3·56 (1)	—O(24)	3·33 (1)
C(70)—O(8)	3·68 (2)	—O(46)	3·39 (1)
		C(6)—O(3)	3·54 (1)
XYL2—framework		—O(17)	3·49 (1)
		C(7)—O(43)	3·39 (1)
C(1)—O(43)	3·49 (1)	C(8)—O(15)	3·67 (1)
C(2)—O(18)	3·46 (1)	—O(28)	3·61 (1)
—O(25)	3·33 (1)		
—O(30)	3·66 (1)	XYL1—XYL2′	
—O(31)	3·61 (1)		
—O(44)	3·32 (1)	C(40)—C(1)′	4·02 (2)
C(3)—O(18)	3·54 (1)	C(40)—C(7)′	4·29 (2)
—O(25)	3·16 (1)	C(50)—C(1)′	3·96 (2)
—O(28)	3·44 (1)	C(50)—C(7)′	3·94 (2)

From a packing analysis of *p*-xylene in H-ZSM-5 (Reischman *et al.*, 1988) the positions of eight independent *p*-xylene molecules, four in each channel system, were predicted. Because of the symmetry of the framework used (*Pnma*), a second set of coordinates related to the first one by *m*, is equally possible. As described above, the interaction forces between XYL2 molecules are very weak. Therefore, a mixture of the two sets of coordinates, just mentioned, might give a possible solution as well. Using the orthorhombic $P2_12_12_1$ symmetry, the eight molecules given by Reischman *et al.* (1988) were transformed to the positions of XYL1 and XYL2. A comparison of Reischman's (transformed) and our fractional coordinates made clear that two of their four molecules in the straight channel and one of their four molecules in the sinusoidal channel were in a mirrored position. After correcting these positions there are minor differences in the position of the centroid of the molecules and the rotational orientations around the long molecular axis. This illustrates the potential strength of the packing-analysis calculations.

A possible sorption mechanism of p-xylene

It is tempting to speculate on the diffusion pathway of *p*-xylene in the zeolite framework given the known frameworks of ORTHO, MONO and PARA and assuming that ORTHO has *Pnma* symmetry. Pore sizes of those 10-rings mainly governing the sieve and diffusion properties (van Koningsveld, Jansen & van Bekkum, 1989), are listed in Table 7. The elliptical cross section of *p*-xylene has, using van der Waals radii, main axes of ~6·1 and 4·0 Å. The reported kinetic diameter is 5·85 Å (Breck, 1974).

p-Xylene has a strong preference for diffusion and adsorption in the straight channels (Derouane & Gabelica, 1980; Eckman & Vega, 1986; Ma, Tang, Sand & Hou, 1986). Above the transition temperature ($T_c \simeq 340$ K), in ORTHO, the two 10-rings in the double 10-ring *within* the (010) pentasil layer are related by $\bar{1}$ and *between* successive (010) layers by *m*. Therefore, the direction of maximal pore size is the same in all 10-rings constituting the straight channel. Diffusion of *p*-xylene in the straight channels of ORTHO may take place mainly through the 4→9 ports. This is in agreement with the orientation of XYL1 at the intersection of channels in PARA, in which XYL1 indeed has its short molecular axis in the 4→9 direction

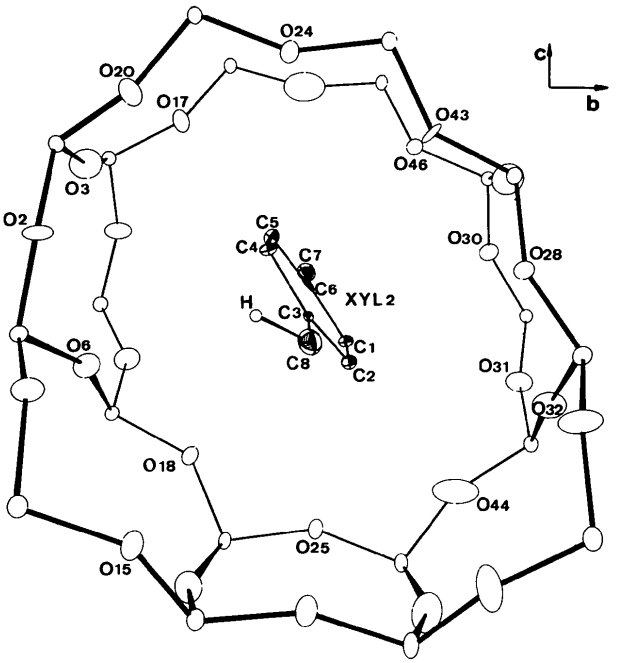

Fig. 5. XYL2-to-framework interactions in the sinusoidal double 10-ring of PARA seen down [100]. (Thermal ellipsoids of XYL2 are scaled down with an arbitrarily chosen factor.)

Table 7. *Pore openings* (O···O *distances*, Å; *e.s.d.'s* ≈ 0·005 Å) *in those* 10*-rings in the straight channel which are related by 'm' in ORTHO and in the double* 10*-rings in the sinusoidal channel*

Maximal and minimal O···O distances are underlined. Max. and min. pore sizes are calculated using 1·35 Å for the O-atom radius. The O numbering is for use in this table only and is defined as given in the diagram below.

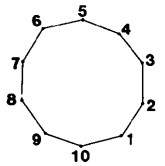

10-rings in the straight channel (*cf.* Fig. 4*a*)

	1→6	2→7	3→8	4→9	5→10	Max.	Min.
ORTHO*	7·922	8·124	8·164	8·449	8·081	5·75	5·22
MONO	8·115	7·875	8·484	8·243	8·086	5·78	5·18
	7·969	8·163	8·532	8·487	7·980	5·83	5·27
PARA	7·774	7·949	8·615	8·755	8·099	6·06	5·07
	7·503	7·968	8·489	8·882	8·071	6·18	4·80

10-rings in the sinusoidal channel (*cf.* Fig. 5)

ORTHO†	8·250	8·132	8·132	8·250	7·992	5·55	5·29
	7·983	8·079	8·079	7·983	8·295	5·60	5·28
MONO	8·593	8·171	8·054	8·113	8·148	5·89	5·35
	8·162	7·712	8·476	7·760	8·400	5·78	5·01
PARA	9·071	8·606	7·578	7·456	8·302	6·37	4·76
	8·846	8·533	7·447	7·278	8·591	6·15	4·58

* Second ring related to first one by *m*.
† There is a mirror plane through O(5) and O(10).

(*cf.* Table 7 and Fig. 4*a*). Below the transition temperature, in MONO, the double 10-ring *within* the (010) layer still has $\bar{1}$ symmetry; *between* successive (010) layers *m* is lost. However, the two independent 10-rings* (Table 7) still have their maximal pore dimension in the same (3→8) direction and so have all 10-rings in the straight channel. The maximum pore size in the straight channel of about 5·8 Å is not affected by the ORTHO–MONO phase transition and is close to the kinetic diameter of *p*-xylene. The cage at the intersection of channels can be reached by diffusion in the straight channel through the 3→8 (and very probably 4→9) ports in MONO. The *p*-xylene molecule entering the cage needs a small reorientation to the observed orientation of XYL1 in PARA. The two 10-rings in PARA become more elliptical with limiting ports of 6·06 × 5·07 and 6·18 × 4·80 Å.

Let us now consider the possibilities of diffusion in the sinusoidal channel. Above T_c the space group of ORTHO is *Pnma* (assumed). In both 10-rings the minimal and maximal pore sizes are 5·3 and 5·6 Å. However, as is seen from Table 7, the directions of the maximal and minimal pore dimensions in both 10-rings are interchanged. The 'effective' pore size, the common maximal diameter, is about 5·3 Å. The double 10-ring pore is nearly circular. Above T_c it will therefore be difficult for *p*-xylene (kinetic diameter 5·85 Å) to enter the sinusoidal channel. This is in agreement with the maximal adsorption capacity of 4 molecules per unit cell observed by Olson *et al.* (1981) at 363 K. On cooling down to below the ORTHO–MONO phase transition, the maximal pore dimension in each of the two 10-rings in the sinusoidal channel increases from 5·55 and 5·60 Å to 5·89 and 5·78 Å (the limiting ports attain equal size in both channel systems). Therefore, the sinusoidal channel in MONO will, in principle, be accessible to *p*-xylene. However, from Table 7 it is seen that, if *p*-xylene enters the sinusoidal double 10-ring with its short molecular axis in the 1→6 direction,† it meets a medium-sized pore opening of 8·16 − 2·70 = 5·46 Å at the adjacent 10-ring of the double 10-ring system. Nevertheless, the crystal structure of PARA shows that XYL2 is able to enter the sinusoidal channel in the expected 1→6 direction (Fig. 5).

The adsorption of *p*-xylene and the transition to the PARA form may well be enhanced by the lattice vibrations. The ORTHO–MONO phase transition has been shown to be ferroelastic (van Koningsveld, Tuinstra *et al.*, 1989). At T_c the stress required to transform the lattice from one to the other ferroelastic domain vanishes. The vibration modes represented by the acoustic transverse phonon branch along **b*** with polarization along **c** will become soft at T_c. The long and short pore sizes in the sinusoidal double 10-ring are periodically interchanged inducing a peristaltic movement of the channel along [010]. The amplitudes of the atomic displacements are relatively large, enhancing the adsorption of *p*-xylene. Once the *p*-xylene molecules have entered the sinusoidal channels, the sinusoidal double 10-ring is deformed to even more elliptical cross sections of 6·37 × 4·76 and 6·15 × 4·58 Å in the two 10-rings, yielding an improved accommodation of the sorbate (cross section ≃ 6·1 × 4·0 Å; note the analogous dimensions in the straight channel in PARA). Through interactions in the pentasil chain, such a deformation initiates a coupled deformation in the four nearest neighbouring double 10-rings in the (100) layer (see Fig. 2*d*).‡ The resulting shift of adjacent (010) layers along **c** is strictly alternating. The twofold screw axis along **c** is restored and the symmetry of the PARA framework becomes $P2_12_12_1$.§

* A minor shift with respect to each other along **c** has been neglected.

† Entering the sinusodail channel *via* the adjacent 10-ring seems less probable because in that case a more complicated pathway of the diffusing *p*-xylene molecule in the straight channel is required.

‡ There is a striking resemblance between this cooperative deformation of 10-rings in the (100) layer of H-ZSM-5 and the proposed deformation of 8-rings in the (001) layer of tetranatrolite compared with the most symmetrical arrangement in natrolite (Gottardi & Galli, 1985).

§ It should be noted that the representation describing a transition from ORTHO to PARA would belong, in the extended zone scheme, to the same phonon dispersion branch as used in describing the ORTHO–MONO transition.

Below T_c an activation energy is required to transform the crystal from MONO to PARA. Since the deformation of the monoclinic angle only amounts to 0·67° (van Koningsveld, Tuinstra *et al.*, 1989) this activation energy is expected to be small and even at temperatures below T_c a shift of neighbouring (010) layers along **c** can be induced by the lattice vibrations.

The cooperative deformation of the (100) pentasil layer may explain the sudden increase of *p*-xylene adsorption near the transition temperature (Olson *et al.*, 1981) and even at 313 K (Richards & Rees, 1988): at constant system composition the solid phase changes from 4 to about 7·6 molecules of *p*-xylene per unit cell. *p*-Xylene molecules, formerly adsorbed at the channel intersections, collectively move to the sinusoidal channels. Subsequently, incoming new *p*-xylene molecules diffuse into the straight channels and are trapped at the channel intersections by establishing the H···C contacts described previously.

After storage for half a year (at 295 K), the PARA crystal was remeasured at 295 K. The symmetry is still $P2_12_12_1$ and no spontaneous desorption of *p*-xylene has taken place. This is in agreement with ^{13}C MAS NMR spectra which show that in a high-loaded *p*-xylene/H-ZSM-5 powder the motion of *p*-xylene is essentially frozen up to 293 K. A slow exchange of sites starts above 293 K (Reischman *et al.*, 1988). Analogous spectra obtained at ~310 K (Nagy, Derouane, Resing & Miller, 1983) were consistent with rapid translational diffusion of the molecules in both channel systems. From the observed *p*-xylene packing in PARA, it can be anticipated that, upon desorption, the *p*-xylene in the straight channels leaves the crystal first. The interaction forces between the methyl (H) atom in XYL2 and the aromatic ring atoms in XYL1, established upon adsorption, have to be surmounted and hysteresis occurs. The leaving *p*-xylene molecules in the straight channel are then replaced by molecules from the sinusoidal channel and desorption continues.

A detailed structural analysis of the 'low-coverage' *p*-xylene/H-ZSM-5 complex is in progress.

References

ANDERSEN, J. R., FOGER, K., MOLE, T., RAJADHYAKSHA, R. A. & SANDERS, J. V. (1979). *J. Catal.* **58**, 114–130.

ANDERSON, M., BOSIO, L., BRUNEAUX-POULLE, J. & FOURME, R. (1977). *J. Chim. Phys.* **74**, 68–73.

BOER, J. L. DE & DUISENBERG, A. J. M. (1984). *Acta Cryst.* A**40**, C-410.

BRECK, D. W. (1974). *Zeolite Molecular Sieves*, pp. 636–637. New York: Wiley.

CROMER, D. T. & MANN, J. B. (1968). *Acta Cryst.* A**24**, 321–324.

DEROUANE, E. G. & GABELICA, Z. (1980). *J. Catal.* **65**, 486–489.

ECKMAN, R. R. & VEGA, A. J. (1986). *J. Phys. Chem.* **90**, 4679–4683.

FYFE, C. A., KENNEDY, G. J., DE SCHUTTER, C. T. & KOKOTAILO, G. T. (1984). *J. Chem. Soc. Chem. Commun.* pp. 541–542.

GOTTARDI, G. & GALLI, E. (1985). *Natural Zeolites*, p. 37. Berlin, Heidelberg: Springer-Verlag.

HAY, D. G. & JAEGER, H. (1984). *J. Chem. Soc. Chem. Commun.* p. 1433.

HAY, D. G., JAEGER, H. & WEST, G. W. (1985). *J. Phys. Chem.* **89**, 1070–1072.

HILL, R. J. & GIBBS, G. V. (1979). *Acta Cryst.* B**35**, 25–30.

JOHNSON, C. K. (1965). *ORTEP*. Report ORNL-3794, revised June 1970. Oak Ridge National Laboratory, Tennessee, USA.

KLINOWSKI, J., CARPENTER, T. A. & GLADDEN, L. F. (1987). *Zeolites*, **7**, 73–78.

KOKOTAILO, G. T., FYFE, C. A., KENNEDY, G. J., GOBBI, G. C., STROBL, H., PASZTOR, C. T., BARLOW, G. E., BRADLEY, S., MURPHY, W. J. & OZUBKO, R. S. (1986). *Pure Appl. Chem.* **58**, 1367–1374.

KONINGSVELD, H. VAN, JANSEN, J. C. & VAN BEKKUM, H. (1987). *Zeolites*, **7**, 564–568.

KONINGSVELD, H. VAN, JANSEN, J. C. & VAN BEKKUM, H. (1989). *Zeolites*. Submitted.

KONINGSVELD, H. VAN, TUINSTRA, F., JANSEN, J. C. & VAN BEKKUM, H. (1989). *Zeolites*, **9**, 253–256.

KONINGSVELD, H. VAN, VAN BEKKUM, H. & JANSEN, J. C. (1987). *Acta Cryst.* B**43**, 127–132.

KONINGSVELD, H. VAN, VAN DEN BERG, A. J., JANSEN, J. C. & DE GOEDE, R. (1986). *Acta Cryst.* B**42**, 491–497.

LERMER, H., DRAEGER, M., STEFFEN, J. & UNGER, K. K. (1985). *Zeolites*, **5**, 131–134.

MA, Y. H., TANG, T. D., SAND, L. B. & HOU, L. Y. (1986). *Proceedings of the 7th International Zeolite Conference, Tokyo, August* 17–22, pp. 531–538. Amsterdam: Elsevier.

MENTZEN, B. F. (1987*a*). *Mater. Res. Bull.* **22**, 337–343.

MENTZEN, B. F. (1987*b*). *Mater. Res. Bull.* **22**, 489–496.

MENTZEN, B. F., BOSSELET, F. & BOUIX, J. (1987). *C. R. Acad. Sci.* **305**, 581–584.

MENTZEN, B. F. & VIGNÉ-MAEDER, F. (1987). *Mater. Res. Bull.* **22**, 309–321.

NAGY, J. B., DEROUANE, E. G., RESING, H. A. & MILLER, G. R. (1983). *J. Phys. Chem.* **87**, 833–837.

OLSON, D. H., KOKOTAILO, G. T., LAWTON, S. L. & MEIER, W. M. (1981). *J. Phys. Chem.* **85**, 2238–2243.

REISCHMAN, P. T., SCHMITT, K. D. & OLSON, D. H. (1988). *J. Phys. Chem.* **92**, 5165–5169.

RICHARDS, R. E. & REES, L. V. C. (1988). *Zeolites*, **8**, 35–39.

STEWART, J. M., KRUGER, G. J., AMMON, H. L., DICKINSON, C. W. & HALL, S. R. (1972). The *XRAY*72 system. Tech. Rep. TR-192. Computer Science Center, Univ. of Maryland, College Park, Maryland, USA.

THAMM, H. (1987). *J. Phys. Chem.* **91**, 8–11.

TOSSELL, J. A. & GIBBS, G. V. (1978). *Acta Cryst.* A**34**, 463–472.

WILLIAMS, D. E. (1969). *Acta Cryst.* A**25**, 464–470.

WILLIAMS, D. E. (1972). *Acta Cryst.* A**28**, 629–635.

WU, E. L., LANDOLT, G. R. & CHESTER, A. W. (1986). *Proceedings of the 7th International Zeolite Conference, Tokyo, August* 17–22, pp. 547–554. Amsterdam: Elsevier.

WU, E. L., LAWTON, S. L., OLSON, D. H., ROHRMAN, A. C. JR & KOKOTAILO, G. T. (1979). *J. Phys. Chem.* **83**, 2777–2781.